

A structural screening approach to ketoamide-based inhibitors of cathepsin K

David G. Barrett,^{a,†} John G. Catalano,^a David N. Deaton,^{a,*} Stacey T. Long,^b
Robert B. McFadyen,^a Aaron B. Miller,^c Larry R. Miller,^d
Kevin J. Wells-Knecht^e and Lois L. Wright^f

^aDepartment of Medicinal Chemistry, GlaxoSmithKline, Research Triangle Park, North Carolina 27709, USA

^bDepartment of World Wide Physical Properties, GlaxoSmithKline, Research Triangle Park, North Carolina 27709, USA

^cDiscovery Research Computational, Analytical, and Structural Sciences, GlaxoSmithKline, Research Triangle Park, North Carolina 27709, USA

^dDepartment of Molecular Pharmacology, GlaxoSmithKline, Research Triangle Park, North Carolina 27709, USA

^eDepartment of Research Bioanalysis and Drug Metabolism, GlaxoSmithKline, Research Triangle Park, North Carolina 27709, USA

^fDiscovery Research Biology, GlaxoSmithKline, Research Triangle Park, North Carolina 27709, USA

Received 21 February 2005; revised 4 March 2005; accepted 7 March 2005

Available online 9 March 2005

Abstract—Several novel ketoamide-based inhibitors of cathepsin K have been identified. Starting from a modestly potent inhibitor, structural screening of P² elements led to 100-fold enhancements in inhibitory activity. Modifications to one of these leads resulted in an orally bioavailable cathepsin K inhibitor.

© 2005 Elsevier Ltd. All rights reserved.

Osteoporosis results from an imbalance in the normally tightly coupled processes of bone formation and bone resorption that maintain skeletal integrity.¹ The decreased bone mass resulting from this disequilibrium increases fracture susceptibility. Bone is resorbed by osteoclasts, which secrete protons and proteases that degrade the mineral and protein components of bone. The C1A family cysteine protease cathepsin K is highly expressed in osteoclasts and can rapidly hydrolyze the major component of bone matrix, type I collagen, in complex with glycosaminoglycans.^{2,3} Secretion of cathepsin K by the osteoclasts begins the degradation of organic bone matrix. These initial resorption components are endocytosed with cathepsin K into the osteoclasts, where further degradation occurs during transcytosis. The resulting bone degradation products are then secreted into the circulation.⁴ The importance

of cathepsin K in the bone remodeling process has been demonstrated in both animals and humans.

Pycnodysostosis, a rare human autosomal recessive trait characterized by short stature, abnormal bone and tooth development, increased bone mineral density, and increased bone fragility, results from mutations in cathepsin K that impair its function.⁵ The phenotype of cathepsin K (–/–) mice is also osteopetrotic.⁶ Furthermore, small molecule inhibitors of cathepsin K have proven efficacious in attenuating bone resorption in animal models of osteoporosis.⁷

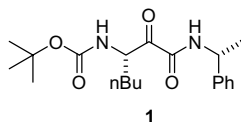
As part of a larger program to develop novel cathepsin K inhibitors for the treatment of osteoporosis, researchers from these laboratories recently reported the discovery of the ketoamide cathepsin K inhibitor **1** (IC₅₀ = 1200 nM).⁸ In addition to a traditional medicinal chemistry approach aimed at replacing the *tert*-butyl group in order to optimize the P²–P³ carbamate's interaction with S²–S³ subsites, a structural screening exercise was also employed.⁹ Since the S² subsite is the deepest, most pronounced hydrophobic binding pocket of the cathepsin K active site, this was perceived to be a fruitful area for structure-based modeling. Furthermore,

Keywords: Ketoamide; Cathepsin K; Cysteine protease inhibitor; Structural screening.

* Corresponding author. Tel.: +1 919 483 6270; fax: +1 919 315 0430; e-mail: david.n.deaton@gsk.com

† Present address: Lilly Forschung GmbH, Essener Str. 93, 22419 Hamburg, Germany.

the cathepsin K S² subsite contains key structural variances versus other human cysteine cathepsin endoproteases, offering opportunities for selectivity versus cathepsins L & S.¹⁰



Structural screening, a reliable, cost effective, and time-saving technique for lead generation/optimization, was employed to diversify the P² substituent for the generation of potential new lead compounds. The Available Chemical Directory (ACD) was selected as the database for screening. The ACD was searched for secondary alcohols that could easily be incorporated into the P² carbamate scaffold. This large set of commercially available chiral and achiral alcohols (~12,000) was then filtered by size (<200 g/mol MW, ~1600) and cost (<\$10/g) parameters. After filtering, the resulting set of alcohols was visually inspected using known cathepsin K crystal structures as a guide.^{11,12} Approximately 25 carbamates were synthesized virtually from these remaining alcohols and docked into a model of the cathepsin K active site derived from an X-ray crystal structure (Brookhaven Protein Data Bank, accession number 1MEM).¹¹ The virtual analogs were attached to the protein via a covalent linkage between the active site thiol ²⁵Cys of cathepsin K and the α -ketone to produce a hemithioacetal. Both stereofacial modes of thiol addition to the ketone were examined. The 'grow' algorithm within the MVP program was used to dock the virtual compounds.¹³ This algorithm 'grows' the virtual molecule one bond at a time and performs a systematic search with each new bond. A minimization was done for each member of the resulting ensemble of docked structures to relax the strain and optimize non-bonded interactions. Then, a scoring function was applied. The active site of cathepsin K was held fixed during the docking process. The covalent nature of these inhibitors makes it difficult to calculate a score. The minimized docked structure energy was compared to its 'unbound' counterpart that only contained ²⁵Cys to represent the hemithioacetal. The modeled P² portions of eight analogs with calculated binding energies comparable to those of inhibitor 1 are shown in Figure 1. The modeled P² moieties that filled more of the S² subsite than the starting *tert*-butyl group were selected for synthesis.

Two general routes were utilized to produce the α -ketoamides. One protocol utilized the Wasserman acyl cyanophosphorane oxidative cleavage and amine coupling procedure to synthesize the ketoamide moiety.¹⁴ As depicted in Scheme 1, commercially available alcohols 2a–e were coupled to the known isocyanate 3.⁸ The resulting carbamates were hydrolyzed to yield acids 4a–e. Coupling of these acids with cyanomethyltriphenylphosphonium ylide gave the phosphoranes 5a–e. Then, oxidative cleavage of the phosphorus–carbon double bond with ozone generated an acyl nitrile. In situ dis-

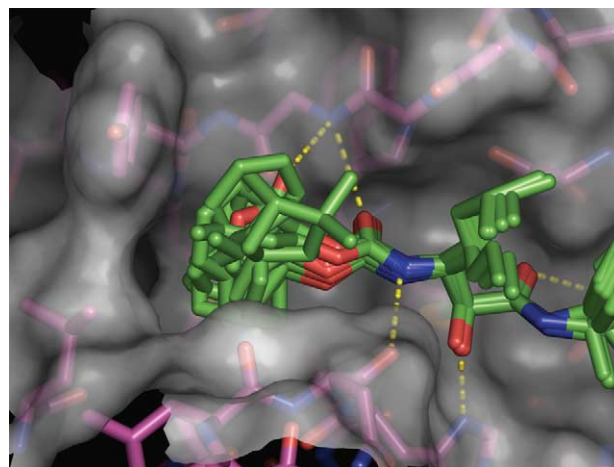
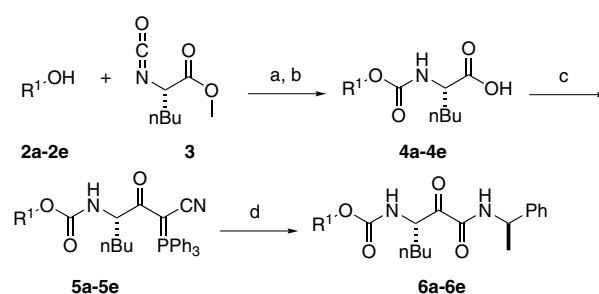


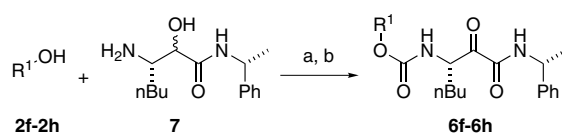
Figure 1. S² subsite of the X-ray crystal structure of cathepsin K with the P² portions of inhibitors 6a–h docked into the enzyme. The cathepsin K carbons are colored magenta with inhibitors 6a–h carbons colored green. The semi-transparent white surface represents the molecular surface, while hydrogen bonds are depicted as yellow dashed lines. This figure was generated using PYMOL version 0.97 (Delano Scientific, www.pymol.org).



Scheme 1. Reagents and conditions: (a) R¹OH, PhMe, 85 °C, sealed tube, 82–99%; (b) LiOH·H₂O, THF, H₂O; 1 N HCl; (c) Ph₃P=CCN, DMAP, EDC, CH₂Cl₂, 35–70% over two reactions; (d) O₃, CH₂Cl₂, –78 °C; N₂; (*R*)- α -methylbenzylamine, –78 °C to rt; AgNO₃, THF, H₂O, 9–32%.

placement of cyanide by (*R*)- α -methylbenzylamine provided the desired ketoamides 6a–e.

The other procedure used to synthesize α -ketoamides involved coupling the chloroformates formed from reaction of the commercially available alcohols 2f–h with phosgene to the known β -amino- α -hydroxy-amide 7.⁸ The resulting carbamates were subsequently oxidized to the desired ketoamides as depicted in Scheme 2.



Scheme 2. Reagents and conditions: (a) R¹OH, 1.93 M COCl₂ in PhMe, pyridine, CH₂Cl₂, –20 °C to rt; 7, iPr₂NEt, dioxane, 22–91%; (b) Dess–Martin periodinane, CH₂Cl₂, 55–78% or TEMPO, 5% NaOCl, KBr, NaHCO₃, CH₂Cl₂, 42–89%.

Gratifyingly, all of the virtual screening derived analogs were more potent than the *tert*-butyl carbamate **1**. The 3,5-dimethyl cyclohexanol derived analogs **6a** ($IC_{50} = 350$ nM) and **6b** ($IC_{50} = 190$ nM) exhibited slight improvements in activity.¹⁵ The indanol analog **6c** was 10-fold more potent than analog **1** ($IC_{50} = 100$ nM), and the tetrahydronaphthol **6d** ($IC_{50} = 32$ nM) was even more active. The norborneol derivative **6e** ($IC_{50} = 26$ nM) was equipotent to **6d**, and the even bulkier fenchyl alcohol derivative **6f** ($IC_{50} = 5.7$ nM) was 4-fold more active than **6e**. The adamantanol analog **6g** ($IC_{50} = 7.2$ nM) and the pantolactone analog **6h** ($IC_{50} = 3.0$ nM) were equipotent to **6f**. The pantolactone derivative **6h** was quite potent despite its reduced size relative to **6f** and **6g**. Furthermore, it was surmised that its increased hydrophilicity relative to the other analogs might result in enhanced aqueous solubility and possibly greater oral exposure. The increased potency presumably arises from the presence of an additional hydrogen bond between the lactone carbonyl and the backbone NH of ⁶⁶Gly in cathepsin K as suggested by the docking calculations.

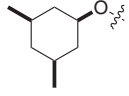
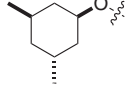
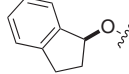
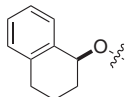
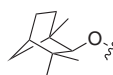
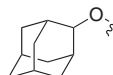
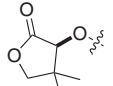
Among the analogs selected for synthesis, no correlation was found between calculated binding energies and measured inhibition constants. This lack of correlation may be in part due to the static nature of the protein active site model, which hampered scoring accuracy by not allowing the protein to expand to accommodate larger substituents such as those found in **6f** and **6g**, resulting in lower scores for these inhibitors. Allowing the enzyme to ‘breathe’, might improve scoring and selection, but would also increase calculation time. Despite these limitations, this structural screening exercise enabled the efficient identification of very potent cathepsin K inhibitors (Table 1).

As shown in Table 2, these analogs were quite selective versus the exopeptidases cathepsin B and cathepsin H. They were less selective versus the more closely related endopeptidase cathepsin L with selectivity ranging from 5 to 360-fold compared to cathepsin K. Selectivity against cathepsins S and V, other closely related endopeptidases, was poor. In fact, analogs **6a** and **6e** were actually more potent cathepsin S inhibitors than cathepsin K inhibitors.

Of the three most active derivatives, analog **6h** was selected for further profiling, because its calculated octanol/water partition coefficient (**6h** ($c\text{Log}P = 5.5$) versus **6f** ($c\text{Log}P = 7.9$) and **6g** ($c\text{Log}P = 7.3$)) was substantially lower than the other ketoamides. As shown in Table 3, **6h** was reasonably soluble in fasted state-simulated intestinal fluid at pH = 6.8 (sol. = 0.24 mg/mL).¹⁶ However, **6h** was cleared extremely rapidly from rat plasma after i.v. dosing in male Han Wistar rats ($C_1 = 460$ mL/min/kg), resulting in a very short terminal half-life ($t_{1/2} = 11$ min). No systemic exposure was seen following p.o. dosing. Plasma stability studies revealed that the lactone of **6h** was rapidly hydrolyzed to the hydroxyacid.

Surmising that in vivo generation of this hydroxyacid might be the cause of the fast clearance of **6h**, the lactam

Table 1. Inhibition of human cathepsin K by P² analogs

#	R ¹	IC ₅₀ ^a (nM)	Calculated binding energy
1		1200	-188.5
6a		350	-193.7
6b		190	-189.7
6c		100	-193.2
6d		32	-194.2
6e		26	-190.5
6f		5.7	-175.4
6g		7.2	-176.2
6h		3.0	-194.5

^a Inhibition of recombinant human cathepsin K activity in a fluorescence assay using 10 μM Cbz-Phe-Arg-AMC as substrate in 100 mM NaOAc, 10 mM DTT, 120 mM NaCl, pH = 5.5. The IC₅₀ values are the mean of two or three inhibition assays, individual data points in each experiment were within a 3-fold range of each other.

6i was synthesized as shown in Scheme 3. Protection of the alcohol of known lactam **8**¹⁷ as the silyl ether, followed by masking of the lactam nitrogen with benzylchloroformate afforded the carbamate **9**. The silyl ether was then cleaved and the resulting alcohol **10** converted into its corresponding chloroformate with phosgene. Coupling to amine **7** and cleavage of the benzyl carbamate yielded **11**. Finally, oxidation of the secondary alcohol **11** provided the ketoamide **6i**.

The lactam **6i** ($IC_{50} = 2.5$ nM) was equipotent to the lactone **6h** ($IC_{50} = 3.0$ nM) and exhibited a similar selectivity profile as well (Table 2). Lactam **6i** was stable in human plasma ($t_{1/2} > 12$ h) and more soluble in FS-SIF than lactone **6h** (sol. **6i** FS-SIF = 0.80 mg/mL vs **6h** FS-SIF = 0.24 mg/mL). The rat pharmacokinetic profile also improved. Although still high, the clearance ($C_1 = 48$ mL/min/kg) was one-tenth that of lactone **6h**, and the terminal half-life ($t_{1/2} = 62$ min) increased

Table 2. Cathepsin B, H, L, S, and V inhibition and selectivity

#	Cat K	Cat B	Cat H	Cat L	Cat S	Cat V
	IC ₅₀ (nM)	IC ₅₀ (nM) ^a	IC ₅₀ (nM) ^b	IC ₅₀ (nM) ^c	IC ₅₀ (nM) ^d	IC ₅₀ (nM) ^e
6a	350	>13,000	>13,000	4400	63	2800
6b	190	>13,000	>13,000	6800	290	2000
6c	100	>13,000	>13,000	460	280	290
6d	32	>2000	>2000	660	79	340
6e	26	>13,000	>13,000	1000	19	190
6f	5.7	12,000	>13,000	1700	30	180
6g	7.2	>5000	>5000	2600	16	390
6h	3.0	>500	>500	410	13	79
6i	2.5	1400	>13,000	150	18	29

^a Inhibition of recombinant human cathepsin B activity in a fluorescence assay using 10 μM Cbz-Phe-Arg-AMC as substrate in 100 mM NaOAc, 10 mM DTT, 120 mM NaCl, pH = 5.5. The IC₅₀ values are the mean of two or three inhibition assays, individual data points in each experiment were within a 2-fold range of each other.

^b Inhibition of recombinant human cathepsin H activity in a fluorescence assay using 50 μM L-Arg-β-naphthalamide as substrate in 100 mM NaOAc, 10 mM DTT, 120 mM NaCl, pH = 5.5.

^c Inhibition of recombinant human cathepsin L activity in a fluorescence assay using 5 μM Cbz-Phe-Arg-AMC as substrate in 100 mM NaOAc, 10 mM DTT, 120 mM NaCl, pH = 5.5.

^d Inhibition of recombinant human cathepsin S activity in a fluorescence assay using 10 μM Cbz-Val-Val-Arg-AMC as substrate in 100 mM NaOAc, 10 mM DTT, 120 mM NaCl, pH = 5.5.

^e Inhibition of recombinant human cathepsin V activity in a fluorescence assay using 2 μM Cbz-Phe-Arg-AMC as substrate in 100 mM NaOAc, 10 mM DTT, 120 mM NaCl, pH = 5.5.

Table 3. Pharmacokinetics of P² analogs

#	cLog P	Sol. FS-SIF ^a (mg/mL)	t _{1/2} ^b (min)	C _l ^c (mL/min/kg)	V _{SS} ^d (mL/kg)	F ^e (%)
6h	5.5	0.24	11	460	3400	0
6i	4.6	0.80	62	48	1300	25

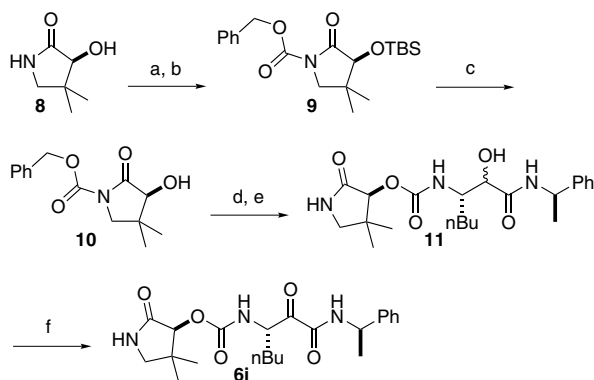
^a FS-SIF is the equilibrium solubility in fasted state-simulated intestinal fluid at pH = 6.8. The values are the mean of two measurements.

^b t_{1/2} is the i.v. terminal half-life dosed as a solution in 15% solutol/citrate buffer at pH 3.5 (2.5 mg/kg) to male Han Wistar rats. All in vivo pharmacokinetic values are the mean of two experiments.

^c C_l is the total clearance.

^d V_{SS} is the steady state volume of distribution.

^e F is the oral bioavailability following a 5.0 mg/kg dose in 15% solutol/citrate buffer at pH 3.5.



Scheme 3. Reagents and conditions: (a) TBSOTf, DMAP, Et₃N, CH₂Cl₂, 48%; (b) NaH, THF, 0 °C; PhCH₂COCl, 0 °C to rt, 94%; (c) TBAF, THF, 94%; (d) R¹OH, 1.93 M COCl₂ in PhMe, pyridine, CH₂Cl₂, -20 °C to rt; **7**, iPr₂NEt, dioxane, 22–91%; (e) H₂/Pd-C, THF, 66%; (f) (COCl)₂, DMSO, CH₂Cl₂, -60 °C; **11**; Et₃N, -60 °C to rt; 56%.

six-fold. More importantly, the lactam **6i** was orally bioavailable (*F* = 25%).

A model of inhibitor **6i** docked into the active site of cathepsin K is shown in Figure 2. The α-keto moiety

of the inhibitor and the active site ²⁵Cys of the enzyme form a covalent hemithioketal intermediate, consistent with the reversible nature of these time dependent, tight binding inhibitors. As shown in ketoamide co-crystal structures from this group,¹⁸ the hemithioketal hydroxyl does not occupy the oxy-anion hole, but rather is stabilized by hydrogen bonds to the catalytic histidine (¹⁶²His) and the backbone carbonyl of ¹⁶¹Asn. Instead, the carbonyl of the amide points into the oxyanion hole where it is stabilized by hydrogen bonds to the side chain NH of ¹⁹Gln and the backbone NH of ²⁵Cys. This differs from the other published aldehyde^{12,19} and ketone²⁰ cathepsin K structures, in which the active site thiol attacks the carbonyl from the opposite face. Two additional hydrogen bonds from the peptide backbone recognition site of the enzyme and the carbamate further stabilize the inhibitor. Thus, the carbamate carbonyl accepts a hydrogen bond from the backbone NH of ⁶⁶Gly, while the carbamate NH donates a hydrogen bond to ¹⁶¹Asn. Another additional hydrogen bond from the carbonyl of the lactam to the backbone NH of ⁶⁶Gly is also present in the model, which may explain the significant potency of this P² group.

Besides these hydrogen bond stabilizing interactions with the protein, the S¹ wall formed from ²³Gly, ²⁴Ser,

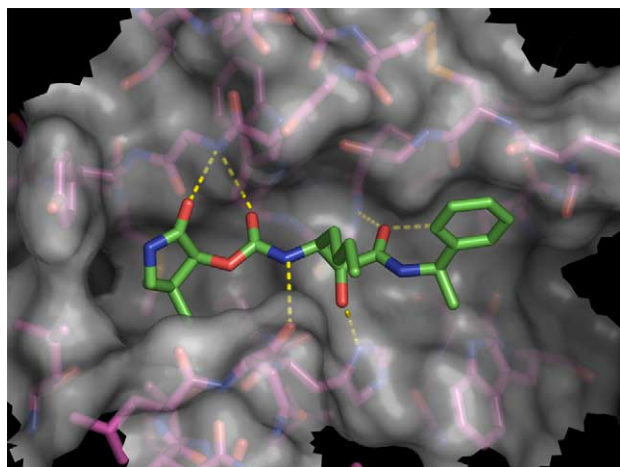


Figure 2. Active site of the model structure of compound **6i** complexed with cathepsin K. The cathepsin K carbons are colored magenta with inhibitor **6i** carbons colored green. The semi-transparent white surface represents the molecular surface, while hydrogen bonds are depicted as yellow dashed lines. This figure was generated using PYMOL version 0.97 (Delano Scientific, www.pymol.org).

⁶⁴Gly, and ⁶⁵Gly abuts the norleucine-derived P¹ group of the inhibitor, with one face of the *n*-butyl group forming van der Waals interactions with the protease while its terminal carbon is solvent exposed. Moreover, the P² lactam forms significant lipophilic interactions with the S² pocket composed of ⁶⁷Tyr, ⁶⁸Met, ¹³⁴Ala, ¹⁶³Ala, and ²⁰⁹Leu. These inhibitors do not contain a P³ element that could potentially interact with the S³ subsite of cathepsin K. Incorporation of P³ groups should enhance inhibitory activity at the cost of increased size of the inhibitor.

In summary, this report showcases a structural screening approach for lead generation. Starting from the ketoamide cathepsin K inhibitor **1**, the P² substituent was replaced with commercially available groups identified through molecular modeling. This exercise produced significant gains in inhibitory activity, including analogs **6f**, **6g**, and **6h**, which were over 100-fold more potent than the starting ketoamide. Modification of inhibitor **6h** produced analog **6i**, which was equipotent and 25% orally bioavailable. Subsequent reports will detail efforts to improve the properties of this series of pantolactone-derived ketoamide-based cathepsin K inhibitors.

References and notes

1. Einhorn, T. A. In *Osteoporosis*; Marcus, R., Feldman, D., Kelsey, J., Eds.; Academic: San Diego, CA, 1996; p 3.
2. Li, Z.; Hou, W.-S.; Escalante-Torres, C. R.; Gelb, B. D.; Bromme, D. *J. Biol. Chem.* **2002**, *277*, 28669.

3. Deaton, D. N.; Kumar, S. *Prog. Med. Chem.* **2004**, *42*, 245.
4. Vaaraniemi, J.; Halleen, J. M.; Kaarlonen, K.; Ylipahkala, H.; Alatalo, S. L.; Andersson, G.; Kaija, H.; Vihko, P.; Vaananen, H. K. *J. Bone Miner. Res.* **2004**, *19*, 1432.
5. Gelb, B. D.; Shi, G.-P.; Chapman, H. A.; Desnick, R. J. *Science* **1996**, *273*, 1236.
6. Kiviranta, R.; Morko, J.; Alatalo, S. L.; NicAmhlaoibh, R.; Risteli, J.; Laitala-Leinonen, T.; Vuorio, E. *Bone* **2005**, *36*, 159.
7. Stroup, G. B.; Lark, M. W.; Veber, D. F.; Bhattacharyya, A.; Blake, S.; Dare, L. C.; Erhard, K. F.; Hoffman, S. J.; James, I. E.; Marquis, R. W.; Ru, Y.; Vasko-Moser, J. A.; Smith, B. R.; Tomaszek, T.; Gowen, M. *J. Bone Miner. Res.* **2001**, *16*, 1739.
8. Catalano, J. G.; Deaton, D. N.; Long, S. T.; McFadyen, R. B.; Miller, L. R.; Payne, J. A.; Wells-Knecht, K. J.; Wright, L. L. *Bioorg. Med. Chem. Lett.* **2004**, *14*, 719.
9. Barril, X.; Hubbard, R. E.; Morley, S. D. *Mini-Rev. Med. Chem.* **2004**, *4*, 779.
10. Somoza, J. R.; Palmer, J. T.; Ho, J. D. *J. Mol. Biol.* **2002**, *322*, 559.
11. McGrath, M. E.; Klaus, J. L.; Barnes, M. G.; Bromme, D. *Nat. Struct. Biol.* **1997**, *4*, 105.
12. Catalano, J. G.; Deaton, D. N.; Furfine, E. S.; Hassell, A. M.; McFadyen, R. B.; Miller, A. B.; Miller, L. R.; Shewchuk, L. M.; Willard, D. H., Jr.; Wright, L. L. *Bioorg. Med. Chem. Lett.* **2004**, *14*, 275.
13. Lambert, M. H. In *Practical Application of Computer-Aided Drug Design*; Charifson, P. S., Ed.; Marcel Dekker: New York, 1997; p 243.
14. Wasserman, H. H.; Petersen, A. K. *Tetrahedron Lett.* **1997**, *38*, 953.
15. Many of the P² moieties in these analogs contain a stereogenic center adjacent to the carbamate. The epimers of these analogs were poor virtual inhibitors of cathepsin K when modeled into the cathepsin K active site.
16. Dressman, J. B.; Amidon, G. L.; Reppas, C.; Shah, V. P. *Pharm. Res.* **1998**, *15*, 11.
17. Kopelevich, V. M.; Bulanova, L. N.; Gunar, V. I. *Tetrahedron Lett.* **1979**, 3893.
18. Tavares, F. X.; Boncek, V.; Deaton, D. N.; Hassell, A. M.; Long, S. T.; Miller, A. B.; Payne, A. A.; Miller, L. R.; Shewchuk, L. M.; Wells-Knecht, K.; Willard, D. H., Jr.; Wright, L. L.; Zhou, H.-Q. *J. Med. Chem.* **2004**, *47*, 588.
19. Boros, E. E.; Deaton, D. N.; Hassell, A. M.; McFadyen, R. B.; Miller, A. B.; Miller, L. R.; Paulick, M. G.; Shewchuk, L. M.; Thompson, J. B.; Willard, D. H., Jr.; Wright, L. L. *Bioorg. Med. Chem. Lett.* **2004**, *14*, 3425.
20. Marquis, R. W.; Ru, Y.; LoCastro, S. M.; Zeng, J.; Yamashita, D. S.; Oh, H.-J.; Erhard, K. F.; Davis, L. D.; Tomvaszek, T. A.; Tew, D.; Salyers, K.; Proksch, J.; Ward, K.; Smith, B.; Levy, M.; Cummings, M. D.; Haltiwanger, R. C.; Trescher, G.; Wang, B.; Hemling, M. E.; Quinn, C. J.; Cheng, H. Y.; Lin, F.; Smith, W. W.; Janson, C. A.; Zhao, B.; McQueney, M. S.; D'Alessio, K.; Lee, C.-P.; Marzulli, A.; Dodds, R. A.; Blake, S.; Hwang, S.-M.; James, I. E.; Gress, C. J.; Bradley, B. R.; Lark, M. W.; Gowen, M.; Veber, D. F. *J. Med. Chem.* **2001**, *44*, 1380.